Bone 120 (2019) 504–511

Contents lists available at ScienceDirect

Bone

journal homepage: www.elsevier.com/locate/bone

Full Length Article

Correction of QCT vBMD using MRI measurements of marrow adipose tissue

Xiaoguang Cheng[a,1], Glen M. Blake[b,*,1], Zhe Guo[a], J. Keenan Brown[c], Ling Wang[a], Kai Li[a], Li Xu[a]

[a] Department of Radiology, Beijing Jishuitan Hospital, Beijing 100035, China
[b] School of Biomedical Engineering & Imaging Sciences, King's College London, St Thomas' Hospital, London SE1 7EH, United Kingdom
[c] Mindways Software Inc., Austin, TX, United States of America

ARTICLE INFO

Keywords:
Quantitative computed tomography
Volumetric bone mineral density
Chemical shift encoded magnetic resonance imaging
Proton density fat fraction
Bone marrow adipose tissue
Bone density accuracy errors

ABSTRACT

Objective: Quantitative computed tomography (QCT) measurements of volumetric bone mineral density (vBMD) are subject to errors due to variations in the amount of bone marrow adipose tissue (BMAT). The purpose of our study was to describe and validate a novel method to correct lumbar spine trabecular vBMD measurements for BMAT using chemical shift-encoded magnetic resonance imaging (CSE-MRI).

Methods: CSE-MRI measurements of proton density fat fraction (PDFF) were used to correct QCT spine vBMD measurements for BMAT based on the H_2O and K_2HPO_4 basis set equivalent densities of bone, red and yellow bone marrow. BMAT corrected and uncorrected vBMD measurements of the L1 vertebra were compared with dual-energy QCT (DEQCT) measurements in 18 subjects (mean age: 68 y, range 60 to 93 y). A further 400 subjects (mean age: 53 y, range 21 to 82 y) had 120 kV_p single-energy QCT and CES-MRI scans of L2–L4 and the data used to simplify the adipose tissue correction by deriving a linear equation between the CSE-MRI vBMD correction and fractional BMAT content.

Results: Application of the CSE-MRI derived vBMD correction changed the bias (95% limits of agreement) compared with DEQCT from 26.7 (11.0 to 42.4) mg/cm^3 to 2.2 (−9.5 to 13.9) mg/cm^3 at 80 kV_p, and from 22.4 (3.3 to 41.6) mg/cm^3 to 2.9 (−12.6 to 18.4) mg/cm^3 at 120 kV_p. Data for the 400 subjects gave the following relationship valid at 120 kV_p: vBMD correction (mg/cm^3) = −12.96 + 75.76 × BMAT.

Conclusion: CSE-MRI measurements of PDFF can be used to correct for BMAT content and improve the accuracy of lumbar spine QCT vBMD measurements calibrated using a K_2HPO_4 phantom.

1. Introduction

Measurement of volumetric bone mineral density (vBMD) using quantitative computed tomography (QCT) plays an important role in the evaluation of patients with osteoporosis and is deemed the gold standard for vBMD assessment [1,2]. However, the accuracy of QCT in assessing vBMD is decreased due to differences in the amount of bone marrow adipose tissue (BMAT) [3,4]. Studies using dual energy QCT (DEQCT) have been performed to assess the influence of BMAT on vBMD measurements [5,6]. However, DEQCT is associated with increased radiation dose and no studies have validated equations for BMAT correction.

Magnetic resonance imaging (MRI) measurements using proton magnetic resonance spectroscopy (^{1}H-MRS) [7,8] or chemical shift-encoded MRI (CSE-MRI) [8,9] are sensitive and accurate non-invasive methods of evaluating BMAT content [10,11]. The purpose of our study was to use CSE-MRI measurements of BMAT to correct the errors in single-energy QCT (SEQCT) lumbar spine trabecular vBMD due to BMAT content and to validate the method in subjects who had DEQCT, SEQCT and CSE-MRI to compare BMAT-corrected vBMD with DEQCT vBMD.

Abbreviations: BM, Bone marrow; BMAT, Bone marrow adipose tissue; CSE-MRI, Chemical shift-encoded MRI; DEQCT, Dual-energy quantitative computed tomography; F_{PDFF}, Symbol for proton density fat fraction; F_{YM}, Symbol for fractional volume of yellow marrow in bone marrow; HU, Hounsfield units; PDFF, Proton density fat fraction; QCT, Quantitative computed tomography; ROI, Region of interest; RM, Red bone marrow; YM, Yellow bone marrow; *X*, Fractional volume of bone in vertebral body ROI; *Y*, Fractional volume of yellow marrow in vertebral body ROI; *Z*, Fractional volume of red marrow in vertebral body ROI

* Corresponding author at: King's College London, Osteoporosis Research Unit, Guy's Campus, London SE1 9RT, United Kingdom.
E-mail address: glen.blake@kcl.ac.uk (G.M. Blake).

[1] Joint first authors.

https://doi.org/10.1016/j.bone.2018.12.015
Received 29 July 2018; Received in revised form 14 December 2018; Accepted 18 December 2018
Available online 21 December 2018

Table 1
Basis set decomposition of bone, red marrow and yellow marrow into equivalent densities of H_2O and K_2HPO_4. The results were derived by one of the authors (JKB) using tissue composition data from ICRU Report 46 [13], typical spectral data for CT scanners, and the National Institute of Standards and Technology (NIST) X-ray attenuation tables [30]. A description of how the equivalent densities were calculated is given in the Appendix.

Tissue	Density (mg/cm^3)	H_2O equivalent density (mg/cm^3)	K_2HPO_4 equivalent density (mg/cm^3)
Bone	1250[a]	727.85	1250.00
Red marrow	1030	1037.15	−12.24
Yellow marrow	930	969.46	−36.57

[a] Density of bone refers to the vBMD of pure cortical bone.

2. Methods

2.1. vBMD measurements and the equivalent densities plot

We assume that the region of interest (ROI) drawn to measure vBMD in vertebral trabecular bone contains three types of tissue, bone, yellow marrow (YM) and red marrow (RM). Let X, Y and Z be the fractional volume of bone, YM and RM respectively. Since only these three tissues are present, $X + Y + Z = 1$. Let F_{YM} represent the fractional volume of YM in bone marrow (BM) [$F_{YM} = Y/(Y + Z)$].

Measurements of CT numbers made in Hounsfield units (HU) are often interpreted by representing the X-ray attenuation properties of tissue in terms of the basis set equivalent densities of water (H_2O) and dipotassium hydrogen phosphate (K_2HPO_4) [12]. We write the basis set equivalent densities of the tissue in the vertebral body trabecular ROI as [$A(H_2O)$, $B(K_2HPO_4)$], where $A(H_2O)$ is the equivalent density of the H_2O component and $B(K_2HPO_4)$ the K_2HPO_4 component, both in units of mg/cm^3. The equivalent densities of bone, YM and RM are listed in Table 1, and an explanation of how these numbers were calculated is given in the Appendix A. The values of $A(H_2O)$ and $B(K_2HPO_4)$ are related to the fractional volumes X, Y and Z by the equations:

$$A(H_2O) = 727.9\,X + 969.5\,Y + 1037.1\,Z \quad (1a)$$

$$B(K_2HPO_4) = 1250.0\,X - 36.6\,Y - 12.2\,Z \quad (1b)$$

The effect of differences in BM composition on the H_2O and K_2HPO_4 equivalent densities is shown schematically in Fig. 1. The point T representing the tissue composition in the vertebral body ROI lies within the triangle PQR whose vertices represent bone, YM and RM respectively. The line FP drawn through T represents the line of constant marrow composition F_{YM} as X varies from 0 to 1.0.

2.2. CT numbers in the equivalent densities plot

In Fig. 1 the CT number at T is related to the equivalent densities [$A(H_2O)$, $B(K_2HPO_4)$] by the following equation [14]:

$$CT = mH\,A(H_2O) + mK\,B(K_2HPO_4) - 1000 \quad (2)$$

where mH and mK are scaling factors (units HU mg^{-1} cm^3) for the H_2O and K_2HPO_4 equivalent densities and 1000 is subtracted to ensure the CT number for water is zero. Given that the density of water is close to 1000 mg/cm^3 and the definition of Hounsfield units in terms of the X-ray attenuation of air and water, then the value of mH is close to 1.0, and for present purposes we assume it is exactly unity. The value of mK varies with changes in the X-ray spectrum and is determined from the vBMD calibration slope derived by scanning a QCT phantom with known standards of K_2HPO_4 [15]:

$$mK = \text{vBMD calibration slope} + 0.2174 \quad (3)$$

where 0.2174 HU mg^{-1} cm^3 reflects the amount of water displaced when K_2HPO_4 is added to a given volume of water in such a manner that the original sample volume is maintained [14]. Once mH and mK in Eq. (2) are known the mean CT number in the vertebral body ROI is represented in Fig. 1 by the straight line H_1H_2. In SEQCT the value of vBMD is uncertain because the tissue composition could lie anywhere along the line H_1H_2 depending on the BM composition. However, if F_{YM} can be determined from a MRI measurement then the point F in Fig. 1 is known and X is found from the intersection of FP and H_1H_2 at T.

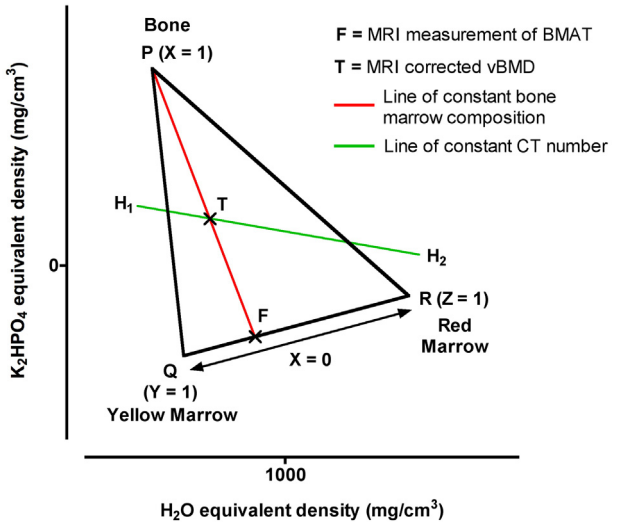

Fig. 1. Schematic explanation of the correction of QCT vBMD measurements for variations in BMAT based on a plot of vertebral body ROI composition represented as H_2O and K_2HPO_4 basis set equivalent densities. The vertices of the triangle PQR represent bone, pure YM and pure RM respectively, and X, Y and Z are the fractional volumes of bone, YM and RM at any point within the triangle. H_1H_2 is the line of constant CT number in the equivalent densities plot based on the QCT measurement in the vertebral body ROI. In the absence of any information about BM composition, the true composition in the vertebral body ROI can lie anywhere between H_1 and H_2. The MRI corrected vBMD measurement is made at T, the point of intersection of H_1H_2 with the line FP, where F is determined by the marrow composition found from a MRI measurement of PDFF. The line FP is a line of constant marrow composition as X varies from 0 to 1.0. The correct value of X is found using F ($X = 0$) and P ($X = 1$) as reference points and scaling the point T along the line FP. Once X is known the value of vBMD is found by multiplying by 1250 mg/cm^3, the nominal vBMD of pure bone (Table 1).
QCT: quantitative computed tomography; vBMD: volumetric bone mineral density; BMAT: bone marrow adipose tissue; ROI: region of interest; H_2O: water; K_2HPO_4: dipotassium hydrogen phosphate; YM: yellow marrow; RM: red marrow; MRI: magnetic resonance imaging; PDFF: proton density fat fraction.

2.3. The calculation of MRI corrected vBMD using CT numbers

Given the linear relationship between CT numbers and equivalent densities in Eq. (2), the value of X at the point T in Fig. 1 can be derived by estimating the CT numbers at F and P and scaling the CT number at T relative to these points:

$$X = \left(\frac{CT_{ROI} - CT_{X=0}}{CT_{X=1} - CT_{X=0}}\right) \quad (4)$$

where CT_{ROI} is the mean CT number measured in the vertebral body ROI, $CT_{X=0}$ the estimated CT number at F (at F the values of X,Y,Z are 0,F_{YM},1-F_{YM}) and $CT_{X=1}$ the estimated CT number at P (at P the values of X,Y,Z are 1,0,0). For pure BM with a YM fractional volume F_{YM} the values of $A(H_2O)$ and $B(K_2HPO_4)$ in Eqs. (1a) and (1b) become:

$$A_{BM}(H_2O) = 969.5\,F_{YM} + 1037.1\,(1 - F_{YM}) \quad (5a)$$

$$B_{BM}(K_2HPO_4) = -36.6\,F_{YM} - 12.2\,(1 - F_{YM}) \quad (5b)$$

and the value of $CT_{X=0}$ at F is found by substituting these equivalent densities in Eq. (2). Similarly the value of $CT_{X=1}$ at P is found by

substituting the equivalent densities of pure bone from Table 1 into Eq. (2). Once X is found using Eq. (4) the MRI corrected vBMD value is found by multiplying X by 1250 mg/cm^3 (Table 1).

2.4. Estimation of the fractional volume of yellow marrow from a PDFF measurement

CSE-MRI scans give a fat measurement referred to as the proton density fat fraction (PDFF) [16], which we denote by F_{PDFF}. A study reported by Goodsitt showed that typically around 95% of marrow fat is located in YM [17]. Studies of phantoms containing fat, water and trabecular bone have reported that PDFF measurements provide an accurate measurement of the fat content of bone marrow [18,19], and other studies suggest a close relationship with the fractional volume of YM [5,20].

Bredella compared ^{1}H-MRS measurements of PDFF in lumbar vertebrae with DEQCT measurements of F_{YM} obtained by projecting the H_2O and K_2HPO_4 equivalent densities onto the BM composition axis QR in Fig. 1 [5]. They found good agreement between F_{YM} and F_{PDFF} with a mean difference of −0.02, 95% limits of agreement (LOA) of −0.24 to +0.20, and a correlation coefficient $r = 0.91$ ($P < 0.001$). This suggests that to sufficient approximation measurements of PDFF can be substituted for F_{YM} in Eqs. (5a) & (5b) to estimate the H_2O and K_2HPO_4 equivalent densities of BM.

This conclusion is supported by a study of goose liver fat published by our group [21]. CSE-MRI measurements of PDFF using the same commercial MRI application (mDIXON-Quant, Philips Healthcare, Best, Netherlands) as that used in the clinical study described in the present paper were made in the livers of geese overfed with corn for periods between 0 and 28 days and compared with Soxhlet extraction measurements of triglyceride content. Linear regression analysis gave the following relationship between the fractional mass of chemically extracted triglyceride and PDFF:

$$\text{Chemically extracted fat fraction} = -0.018 + 0.773 \times \text{PDFF} \quad (6)$$

The small intercept and the slope consistent with the fractional fat content of adipose tissue recommended by the Task Group on Reference Man [22] suggests that the mDIXON-Quant PDFF measurements in this study were a good approximation to the adipose tissue fraction in liver. For measurements of bone marrow the BMAT fraction approximates to the YM fraction (Table 2).

2.5. Comparison of MRI corrected vBMD with DEQCT vBMD

The reliability of using PDFF measurements to correct SEQCT vBMD measurements for BMAT was evaluated in a DEQCT study. A sample size calculation showed that a study with 18 subjects would have 90% power to verify a statistically significant correlation between the MRI and DEQCT derived vBMD corrections with a Type-1 error of P = 0.05. The subjects were recruited from communities living near the Beijing Jishuitan Hospital enrolled as healthy controls in the China Action on Spine and Hip Status (CASH) study [23]. The DEQCT study was approved by the hospital's IRB and all subjects gave written informed consent.

Scans at 80 and 120 kV_p of the L1 lumbar vertebra were performed using a Toshiba CT scanner (Aquilion PRIME ESX-302A, Toshiba Medical Systems Corporation, Ōtawara, Japan) with the subject in a supine position. Subjects were scanned with a Mindways solid calibration phantom (Mindways Software Inc., Austin, TX, USA) calibrated to aqueous K_2HPO_4 vBMD. Mindways QCT Pro analysis software was used to measure SEQCT vBMD values for the 80 and 120 kV_p scans in a 9 mm thick elliptical ROI in trabecular bone in the middle plane of the L1 vertebral body (Fig. 2A). DEQCT vBMD measurements were calculated from the intersection of the lines of constant CT number at 80 and 120 kV_p in Fig. 1. DEQCT measurements of marrow adipose tissue were calculated by projecting a line drawn through P and the point of intersection of the DEQCT measurements onto the line QR in Fig. 1.

On the same day the subjects also underwent a lumbar spine CSE-MRI mDIXON-Quant study on a 3.0 T scanner (Ingenia, Philips Healthcare, Best, Netherlands). The mDIXON sequence is a 3D-FFE sequence, and uses multiple acquired echoes to generate water, fat, T2*, R2*, and in-phase and opposed-phase images synthesized from the water-fat images [24]. The scan parameters of the single breath-hold mDIXON-Quant were as follows: repetition time (TR) = 9.1 ms; first echo time (TE1) = 1.33 ms; 6 echoes with TE shift (ΔTE) = 1.3 ms; field of view = 180 × 140 × 90 mm^3; flip angle = 3°; voxel size = 2.5 × 2.5 × 3.0 mm^3; sensitivity encoding = 2; number of signal averages = 2; and scan time = 12.5 s. After acquisition the images were transferred to an ISP V7 workstation (Philips Healthcare, Best, Netherlands) and the fat content of L1 measured in an identical ROI to the DEQCT study (Fig. 2B). The scans were analysed by an experienced radiologist (ZG). MRI corrected values of vBMD were calculated using Eqs. (2) to (5b) with the approximation $F_{YM} \approx F_{PDFF}$.

2.6. Development of a simple equation to correct vBMD for BMAT

To examine more closely the relationship between the vBMD correction and BMAT we studied subjects enrolled in two on going observational studies at our institution. Two hundred and fifty three subjects (156 women, 97 men) aged between 43 and 82 y were enrolled as part of the international Prospective Urban Rural Epidemiology (PURE) Study and were scanned at their 9-year visit. Recruitment criteria of PURE study subjects in China were published previously [25]. Inclusion criteria were that participants should be aged over 40 y old and able to give informed consent. Exclusion criteria were pregnant women, individuals with metal implants in the lumbar spine, and use of medications or the existence of any disease or condition known to influence bone density. Another 147 subjects (77 women, 70 men) aged between 21 and 52 y were enrolled in a population study to investigate the sex- and age-stratified normative vBMD values of the cervical vertebrae by QCT and determine correlations with the lumbar vertebrae [26]. Inclusion criteria were healthy adults aged 20–65 y and resident in Beijing for > 5 years. Exclusion criteria were any disease that may influence bone metabolism, including trauma and tumour, and those taking bone metabolism regulating drugs.

The additional QCT and MRI scans were approved by the hospital's IRB and all subjects gave written informed consent. QCT scans of the lumbar vertebra L2–L4 at 120 kV_p and CSE-MRI scans of the same vertebrae (Fig. 2A,B) were acquired and analysed as described above for the DEQCT study and the MRI corrected vBMD values for each vertebra calculated using Eq. 4. Finally, the BMAT measurements in the three individual vertebrae were averaged to give the mean BMAT for L2–L4, and similarly the mean uncorrected vBMD at 120 kV_p and the mean MRI corrected vBMD, Uncorrected vBMD was subtracted from the MRI corrected vBMD to give the mean vBMD correction in each subject.

2.7. Statistical analysis

For the 18 subjects in the DEQCT study, scatter and Bland-Altman (BA) [27] plots were drawn examining the relationships between: (1) uncorrected SEQCT vBMD measurements at 80 and 120 kV_p plotted against the corresponding DEQCT vBMD measurement; (2) MRI corrected SEQCT vBMD measurements at 80 and 120 kV_p plotted against

Table 2
Composition of red and yellow bone marrow [17].

Tissue	Fat	Water	Protein	Minerals
Red marrow	3%–6%	82%–86%	6%–8%	0.5%–1.0%
Yellow marrow	71%–92%	7%–26%	1%–2%	0.2%–0.4%

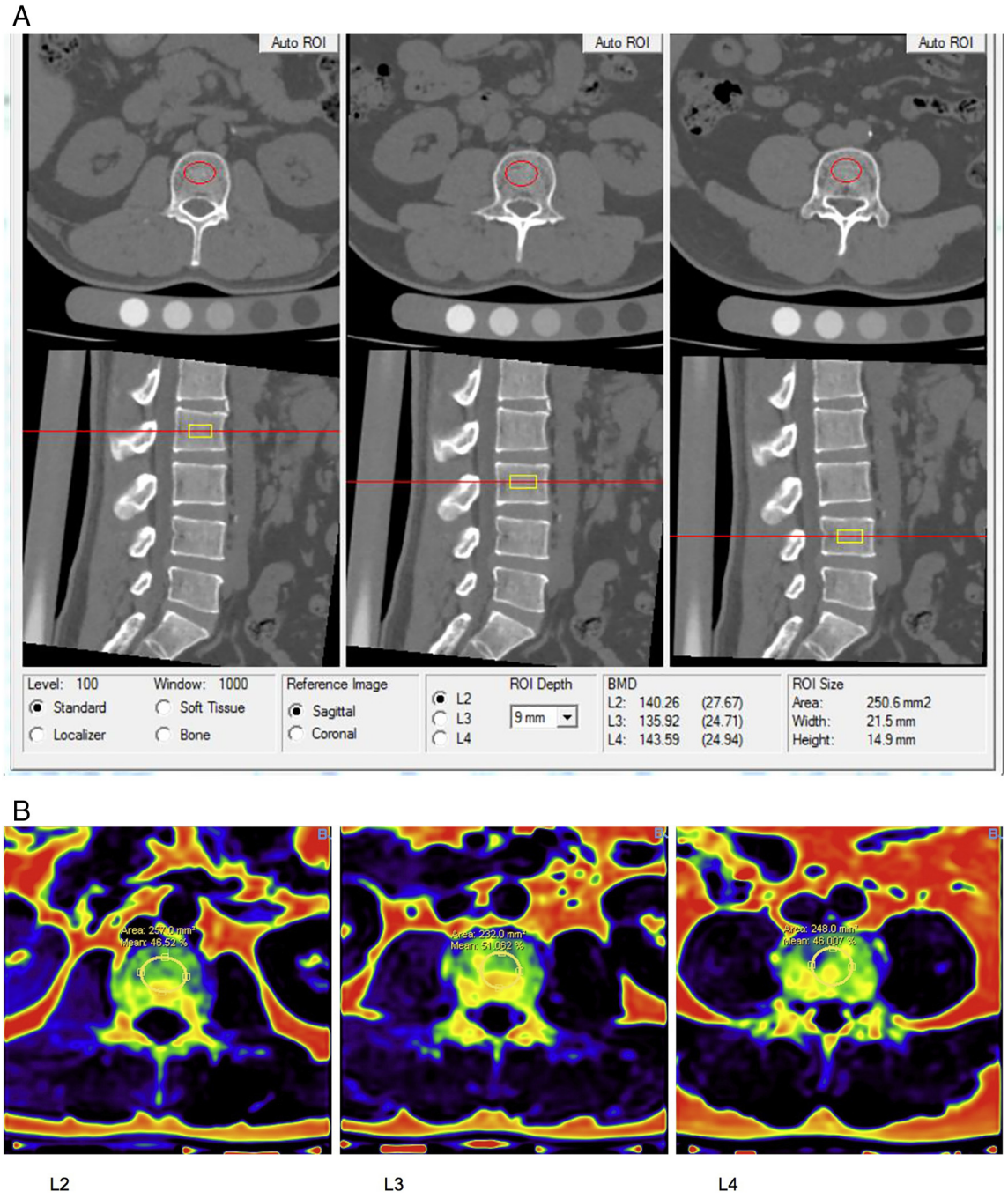

Fig. 2. (A) QCT scan of L2–L4 showing placement of the regions of interest.
(B) CSE-MRI scans of L2–L4 in the same subject showing placement of matching regions of interest.

the DEQCT vBMD measurement. The correlation coefficients of the scatter plots and the bias and 95% LOA of the BA plots were evaluated.

For the 400 subjects in the 120 kV_p QCT study the mean vBMD correction in L2–L4 was plotted against the mean BMAT in the same vertebrae and the data analysed by linear regression to derive the best straight line fit.

A P-value of < 0.05 was taken to be statistically significant.

3. Results

DEQCT and CSE-MRI scans were performed in 18 individuals (11 F, 7 M) with a mean age of 68 years (range 60–93 years). Mean PDFF was 0.51 (range 0.39–0.65) compared with a mean fractional volume of YM in BM of 0.48 (range 0.23–0.63) measured by DEQCT. The PDFF and DEQCT measurements of marrow adipose tissue were significantly correlated ($r = 0.66$; $P = 0.0014$). BA analysis showed a bias (95% LOA) of 0.03 (-0.14 to 0.19).

Plots of the uncorrected vBMD measurements at 80 and 120 kV_p against the DEQCT measurement were highly correlated, although both regression lines departed substantially from the line of identity (Fig. 3). Plots of the MRI corrected vBMD measurements at 80 and 120 kV_p against the DEQCT measurement were similarly correlated and both sets of points lay close to the line of identity (Fig. 4A,B), while the 95% LOA in the BA plots (Fig. 4C,D) were narrower than those in Fig. 3.

For 400 subjects in the 120 kVp QCT study (233 F, 167 M) with a mean age of 53 y (range 21 to 82 y) the plot of the L2–L4 vBMD

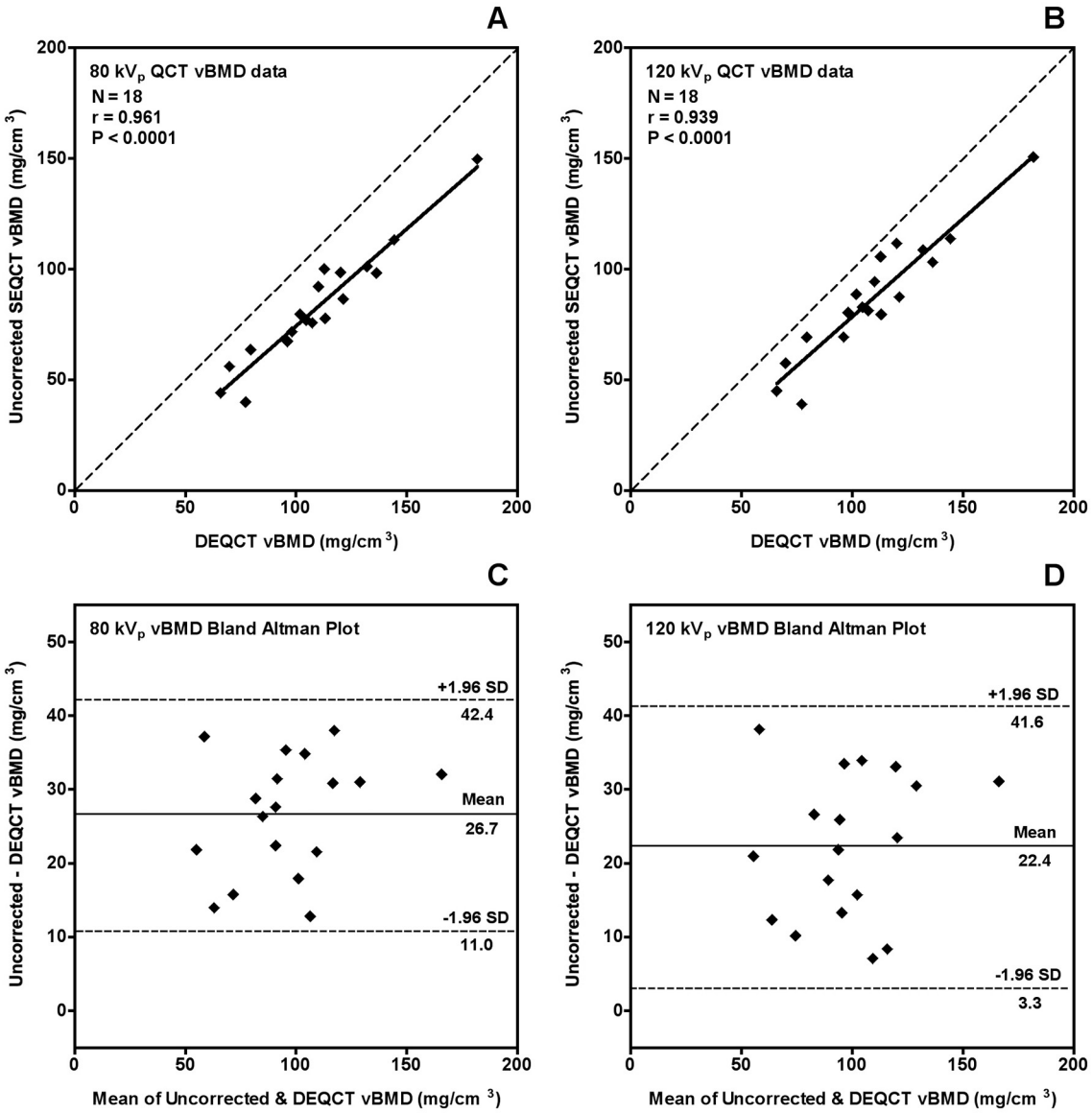

Fig. 3. (A) Scatter plot of the uncorrected SEQCT vBMD measurements at 80 kV_p against the DEQCT vBMD measurements. The continuous line is the linear regression fit. The dashed line is the line of identity.
(B) The same plot for the 120 kV_p vBMD measurements.
(C) The data points in (A) shown as a Bland-Altman plot.
(D) The data points in (B) shown as a Bland-Altman plot.
SEQCT: single-energy quantitative computed tomography; vBMD: vBMD: volumetric bone mineral density. DEQCT: dual-energy quantitative computed tomography.

correction against the BMAT fraction showed a close fit to a straight line (Fig. 5) with the following linear regression fit:

$$\text{vBMD correction (mg/cm3)} = -12.96 + 75.76 \times \text{BMAT} \quad (7)$$

4. Discussion

Measurements of BMAT using CSE-MRI can be used to correct QCT vBMD for differences in BMAT as long as PDFF is a valid measure of the YM fractional volume. Bredella compared ^{1}H-MRS PDFF with DEQCT measurements in vertebral trabecular bone in 12 subjects and demonstrated that, within the 95% LOA of approximately ± 0.2, PDFF was a good approximation to the YM fractional volume measured by DEQCT [5]. Our own DEQCT study in 18 subjects reported here gave similar findings.

A comparison of Figs. 3 and 4 shows that our MRI corrected vBMD measurements are in substantially better agreement with the DEQCT measurements than the uncorrected SEQCT measurements at 80 and 120 kV_p. The close linear relationship between the MRI derived vBMD correction and BMAT measurements demonstrated in Fig. 5 provides a straightforward way of applying the correction to the L2–L4 vertebrae for QCT scans acquired at 120 kV_p and calibrated with the Mindways K_2HPO_4 phantom.

Although the effects of BMAT content can be corrected using DEQCT [5,6], in the past this technique has never achieved a significant clinical role due to the increased radiation dose, reduced reproducibility and the lack of any necessity to correct vBMD measurements for marrow fat content in the routine clinical use of QCT to diagnose osteoporosis. More recently, dual-energy CT scanners have been introduced and shown to have advantages over conventional CT imaging in numerous clinical applications, including bone densitometry [28,29]. Magnetic resonance scanning is also a sensitive and accurate method of measuring the fat content of tissue, and the ^{1}H-MRS technique [7,8] has been widely applied to determine BMAT content in the

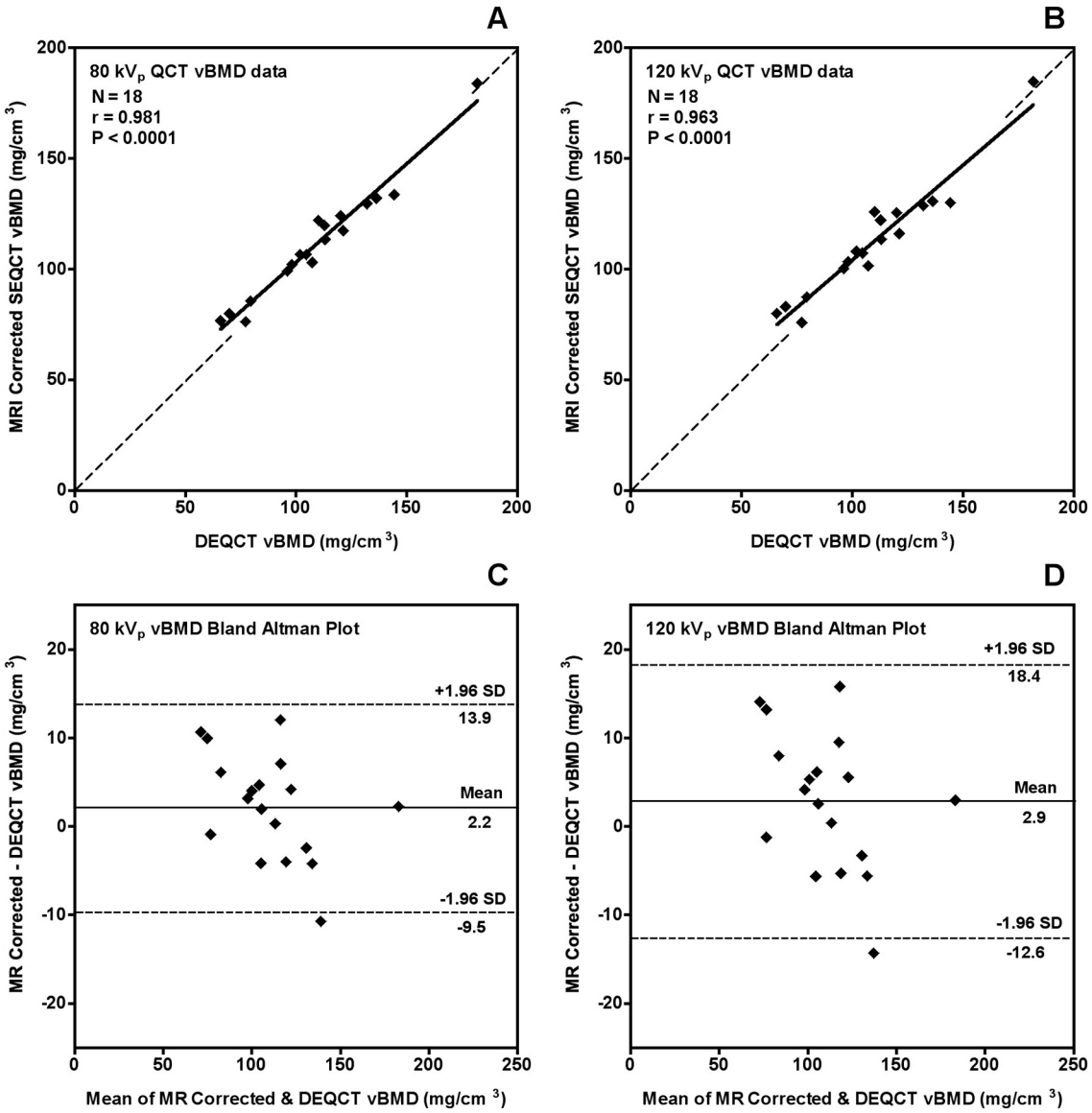

Fig. 4. (A) Scatter plot of the MRI corrected SEQCT vBMD measurements at 80 kV_p against the DEQCT vBMD measurements. The continuous line is the linear regression fit. The dashed line is the line of identity.
(B) The same plot for the 120 kV_p vBMD measurements.
(C) The data points in (A) shown as a Bland-Altman plot.
(D) The data points in (B) shown as a Bland-Altman plot.
MRI: magnetic resonance imaging; SEQCT: single-energy quantitative computed tomography; vBMD: volumetric bone mineral density; DEQCT: dual-energy quantitative computed tomography.

spine. However, ^{1}H-MRS is time-consuming, and now with a newer technique, CSE-MRI, the fat content of human tissue can be assessed quickly and accurately at sites that include the liver and spine with scan times of < 10 min, including patient setup [9,10,21].

For clinical QCT scans for the diagnosis of osteoporosis there is general agreement that it is safe to ignore the errors in vBMD measurements caused by variations in marrow composition [4]. It is not our intention in this paper to challenge this consensus. Our interest in correcting single-energy QCT vBMD measurements using CSE-MRI measurements of marrow composition is to use this technique as a research tool to improve understanding of the relationship between true vBMD and marrow adipose tissue content using data from a large epidemiological study.

Two important considerations for any application of the vBMD correction proposed here are how accurate is the assumption that MRI measurements of PDFF can be equated to the adipose tissue fraction in bone marrow and what consequences do errors in this assumption have in terms of residual errors in the corrected vBMD results? In the Bland-Altman plot between MRI measurements of PDFF and DEQCT measurements of F_{YM} in 12 subjects reported by Bredella et al. [5] the bias (MRI - QCT) was −0.02 with 95% LOA of ± 0.22 about the mean. Our own findings in the 18 subjects reported here were similar, with a bias of +0.03 and 95% LOA of ± 0.17. From the slope of the vBMD correction equation reported here (Fig. 5) the 95% LOA of around ± 0.20 in the Bland-Altman plots cited above results in a ± 1.96 SD error in the vBMD correction of ± 15 mg/cm^3. This is the error when the correction is applied to results in individual patients and is a maximum value for the error, since some of the scatter in the Bland-Altman plot will be due to random errors in the MRI and DEQCT measurements of marrow adipose tissue. As emphasised above, it is not our intention to challenge the established consensus that when making the diagnosis of osteoporosis in individual patients the errors in vBMD measurements

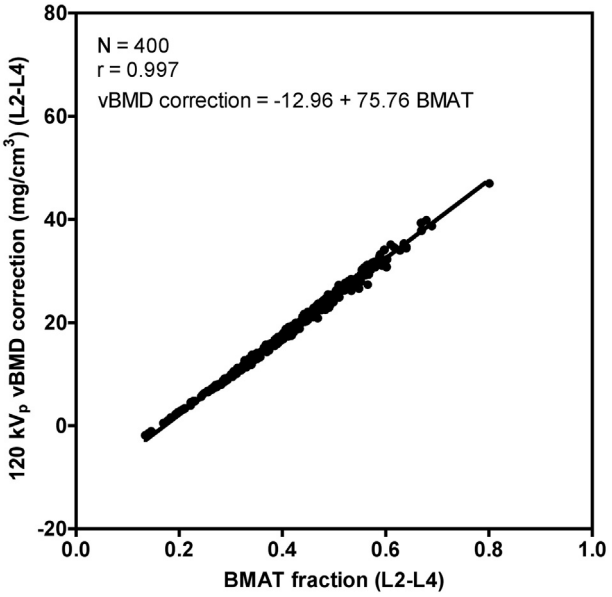

Fig. 5. Scatter plot of the MRI derived vBMD correction at 120 kV_p plotted against BMAT. The data are for 400 healthy Chinese subjects aged 21 to 82 y. The continuous line is the linear regression fit. The MRI vBMD correction can be derived from a measurement of the fractional BMAT using the equation: vBMD correction (mg/cm^3) = $-12.96 + 75.76 \times$ BMAT.
MRI: magnetic resonance imaging; vBMD: volumetric bone mineral density; BMAT: bone marrow adipose tissue.

caused by variations in marrow composition can be ignored [4]. Rather we wish to provide a tool for correcting epidemiological data in large groups of subjects. In this case the relevant consideration is not the 95% LOA in the Bland-Altman plots, but the standard error of the mean in the bias. With the numbers of subjects in the Bland-Altman plot [5] this gives a ± 1.96 SEM of around ± 5 mg/cm^3.

An important limitation of the present study is that the equivalent densities of bone, YM and RM listed in Table 1 and used in Eqs. (1a) through (5b) apply only to QCT scans calibrated with the Mindways K_2HPO_4 phantom. In addition, the simplified correction equation presented in Fig. 5 applies only to QCT scans acquired at 120 kV. At other X-ray tube voltages, scans calibrated with the Mindways phantom can still be corrected using Eqs. (1a)–(5b). For QCT scans calibrated with alternative phantoms, for example those containing hydroxyapatite, the technique illustrated in Fig. 1 may still be used, but the equivalent densities listed in Table 1 and plotted as the vertices of the triangle *PQR* in Fig. 1 require recalculation for the atomic composition of the relevant bone standard. Other limitations include the small number of subjects in the DEQCT study. Our subjects were older (63 to 93 years) than the subjects in the Bredella study (24 to 60 years) and the range of PDFF values were narrower (0.39 to 0.65 compared to 0.26 to 1.04) [5]. Finally, our method of generating the correction is based on the equivalent densities estimated from the YM and RM tissue composition data in ICRU Report 46 [14], and ignores differences in YM and RM composition that may exist between different individuals.

In conclusion, we have described and validated a method of using CSE-MRI measurements to correct spine vBMD measurements for differences in BMAT. When applied to epidemiological datasets it will provide a more reliable understanding of the relationship between BMAT and vBMD and a new tool for the fundamental study of the relationship between bone marrow composition and bone mass.

Disclosures

XC, GMB, ZG, LW, KL and LX have nothing to declare. JKB is a stockholder and employee of Mindways Software, Inc.

Acknowledgements

XC acknowledges financial support from the Beijing Bureau of Health 215 program (grant number: 2009-2-03) and from the Capital Characteristic Clinic Project (grant number: 2014-2-1122). GMB acknowledges support from the Wellcome/EPSRC Centre for Medical Engineering [WT 203148/Z/16/Z]

Appendix A

This appendix describes the calculation of the H_2O and K_2HPO_4 equivalent densities of cortical bone, red marrow and yellow marrow listed in Table 1. We start with the data on the elemental composition of body tissues listed in ICRU Report 46 [13]. For example, for yellow marrow the elemental composition by mass is given as: H 11.5%; C 64.4%; N 0.7%; O 23.1%; Na 0.1%; S 0.1%; Cl 0.1%. From these numbers and the density of yellow marrow (930 mg/cm^3), the contribution of each element to the total density can be calculated. For example, for carbon this is $0.644 \times 930 = 599$ mg/cm^3. The next item of information required is the listing by photon energy of the X-ray mass attenuation coefficients (μ_m units cm^2/g) of the elements in the National Institute of Standards and Technology (NIST) database [30]. CT scan measurements in Hounsfield units represent the X-ray linear attenuation coefficient (μ_L units cm^{-1}) of body tissues. By multiplying the mass attenuation coefficient of carbon at each photon energy by the density of the element in the tissue we derive the contribution of carbon to the linear attenuation coefficient, and by summing over all the elements in the tissue we obtain the total linear attenuation coefficient as a function of X-ray energy. To evaluate the equivalent densities listed in Table 1 we also need to know the mass attenuation coefficients of H_2O [$\mu_m(H_2O)$] and K_2HPO_4 [$\mu_m(K_2HPO_4)$]. The mass attenuation coefficient of H_2O is listed in the NIST database [30], and that of K_2HPO_4 can be calculated by summing the mass attenuation coefficients of the individual elements after multiplying by their fractional contribution to the molecular weight of the compound. With this information, the H_2O equivalent density (*A*) and the K_2HPO_4 equivalent density (*B*) in Table 1 can be found by using least squares regression to fit values of *A* and *B* to the equation:

$$\mu_L(\text{body tissue}) = A\,\mu_m(H_2O) + B\,\mu_m(K_2HPO_4) \quad \text{(A1)}$$

taking values of μ_L(body tissue), $\mu_m(H_2O)$ and $\mu_m(K_2HPO_4)$ at multiple photon energies over an appropriate range (say 30 to 150 keV). Because of the principle of basis set decomposition, the values of *A* and *B* are insensitive to the exact choice of energies.

References

[1] K. Engelke, J.E. Adams, G. Armbrecht, P. Augat, C.E. Bogado, M.L. Bouxsein, D. Felsenberg, M. Ito, S. Prevrhal, D.B. Hans, E.M. Lewiecki, Clinical use of quantitative computed tomography and peripheral quantitative computed tomography in the management of osteoporosis in adults: the 2007 ISCD official positions, J. Clin. Densitom. 11 (2008) 123–162.
[2] C.C. Gluer, Quantitative computed tomography in children and adults, in: C.J. Rosen (Ed.), Primer on the Metabolic Bone Diseases and Disorders of Mineral Metabolism, Eighth edition, John Wiley & Sons, 2013, pp. 264–282.
[3] C.C. Glüer, U.J. Reiser, C.A. Davis, B.K. Rutt, H.K. Genant, Vertebral mineral

determination by quantitative computed tomography (QCT): accuracy of single and dual energy measurements, J. Comput. Assist. Tomogr. 12 (1988) 242–258.
[4] C.C. Glüer, H.K. Genant, Impact of marrow fat on accuracy of quantitative CT, J. Comput. Assist. Tomogr. 13 (1989) 1023–1035.
[5] M.A. Bredella, S.M. Daley, M.K. Kalra, J.K. Brown, K.K. Miller, M. Torriani, Marrow adipose tissue quantification of the lumbar spine by using dual-energy CT and single-voxel ^{1}H-MR spectroscopy: a feasibility study, Radiology 277 (2015) 230–235.
[6] J.G. Sfeir, M.T. Drake, E.J. Atkinson, S.J. Achenbach, J.J. Camp, A.J. Tweed, L.K. McCready, L. Yu, M.C. Adkins, S. Amin, S. Khosla, Evaluation of cross-sectional and longitudinal changes in volumetric bone mineral density in postmenopausal women using single- versus dual-energy quantitative computed tomography, Bone 112 (2018) 145–152.
[7] X. Li, D. Kuo, A.L. Schafer, A. Porzig, T.M. Link, D. Black, A.V. Schwartz, Quantification of vertebral bone marrow fat content using 3 Tesla MR spectroscopy: reproducibility, vertebral variation, and applications in osteoporosis, J. Magn. Reson. Imaging 33 (2011) 974–979.
[8] H.H. Hu, H.E. Kan, Quantitative proton MR techniques for measuring fat, NMR Biomed. 26 (2013) 1609–1629.
[9] T. Baum, S.P. Yap, M. Dieckmeyer, S. Ruschke, H. Eggers, H. Kooijman, E.J. Rummeny, J.S. Bauer, D.C. Karampinos, Assessment of whole spine vertebral bone marrow fat using chemical shift-encoding based water-fat MRI, J. Magn. Reson. Imaging 42 (4) (2015 Oct) 1018–1023.
[10] G. Li, Z. Xu, H. Gu, X. Li, W. Yuan, S. Chang, J. Fan, H. Calimente, J. Hu, Comparison of chemical shift-encoded water-fat MRI and MR spectroscopy in quantification of marrow fat in postmenopausal females, J. Magn. Reson. Imaging 45 (2017) 66–73.
[11] D.C. Karampinos, S. Ruschke, M. Dieckmeyer, M. Diefenbach, D. Franz, A.S. Gersing, R. Krug, T. Baum, Quantitative MRI and spectroscopy of bone marrow, J. Magn. Reson. Imaging 47 (2018) 332–353.
[12] W. Kalender, K. Engelke, T. Fuerst, C.-C. Glüer, P. Laugier, J. Shepherd, ICRU Report 81: quantitative aspects of bone densitometry, J. ICRU 9 (1) (2009).
[13] ICRU Report 46, Photon, Electron, Proton and Neutron Interaction Data for Body Tissues, International Commission on Radiation Units and Measurements, Bethesda, 1992, pp. 11–13. Appendix A.
[14] X. Cheng, G.M. Blake, J.K. Brown, Z. Guo, J. Zhou, F. Wang, L. Yang, X. Wang, L. Xu, The measurement of liver fat from single-energy quantitative computed tomography scans, Quant. Imaging Med. Surg. 7 (2017) 281–291.
[15] X.G. Cheng, K. Li, S.X. Ou, G.Y. Tang, Q.Q. Wang, C. Wang, L. Wang, W. Tian, Heterogeneity in spinal bone mineral density among young adults from three eastern provincial capital cities in mainland China, J. Clin. Densitom. 20 (2017) 198–204.
[16] H.H. Hu, Y. Li, T.R. Nagy, M.I. Goran, K.S. Nayak, Quantification of absolute fat mass by magnetic resonance imaging: a validation study against chemical analysis, Int. J. Body Compos. Res. 9 (2011) 111–122.
[17] M.M. Goodsitt, P. Hoover, M.S. Veldee, S.L. Hsueh, The composition of bone marrow for a dual-energy quantitative computed tomography technique. A cadaver and computer simulation study, Investig. Radiol. 29 (1994) 695–704.
[18] C.S. Gee, J.T. Nguyen, C.J. Marquez, J. Heunis, A. Lai, C. Wyatt, M. Han, G. Kazakia, A.J. Burghardt, D.C. Karampinos, J. Carballido-Gamio, R. Krug, Validation of bone marrow fat quantification in the presence of trabecular bone using MRI, J. Magn. Reson. Imaging 42 (2015) 539–544.
[19] T.J.P. Bray, A. Bainbridge, S. Punwani, Y. Ioannou, M.A. Hall-Craggs, Simultaneous quantification of bone edema/adiposity and structure in inflamed bone using chemical shift-encoded MRI in spondyloarthritis, Magn. Reson. Med. 79 (2) (2018 Feb) 1031–1042.
[20] A. Cohen, W. Shen, D.W. Dempster, H. Zhou, R.R. Recker, J.M. Lappe, A. Kepley, M. Kamanda-Kosseh, M. Bucovsky, E.M. Stein, T.L. Nickolas, E. Shane, Marrow adiposity assessed on transiliac crest biopsy samples correlates with noninvasive measurement of marrow adiposity by proton magnetic resonance spectroscopy (^{1}H-MRS) at the spine but not the femur, Osteoporos. Int. 26 (2015) 2471–2478.
[21] L. Xu, Y. Duanmu, G.M. Blake, C. Zhang, Y. Zhang, K. Brown, X. Wang, P. Wang, X. Zhou, M. Zhang, C. Wang, Z. Guo, G. Guglielmi, X. Cheng, Validation of goose liver fat measurement by QCT and CSE-MRI with biochemical extraction and pathology as reference, Eur. Radiol. 28 (2018) 2003–2012.
[22] W.S. Snyder, M.J. Cook, E.S. Nasset, L.R. Karhausen, G. Parry Howells, I.H. Tipton, Report of the Task Group on Reference Man, Pergamon, Oxford, UK, 1975, p. 43.
[23] K. Li, Y. Zhang, L. Wang, Y.Y. Duanmu, W. Tian, H. Chen, L. Yin, J. Bo, Y. Wang, W. Li, L. He, W.H. Zhao, S.Q. Xu, L.F. Zhao, J. Zhou, F.Z. Wang, Y. Liu, L. Zhu, Y.Z. Chen, X.L. Zhang, X.G. Hao, Z.W. Shi, J.Y. Wang, J.M. Shao, Z.J. Chen, R.S. Lei, G. Ning, Q. Zhao, Y.H. Jiang, Y.H. Zhi, B.Q. Li, X. Chen, Q.Y. Xiang, L. Wang, Y.Z. Ma, S.W. Liu, X.G. Cheng, The protocol for the prospective urban rural epidemiology China action on spine and hip status study, Quant. Imaging Med. Surg. 8 (2018) 667–672.
[24] Y. Zhang, Z. Zhou, C. Wang, X. Cheng, L. Wang, Y. Duanmu, C. Zhang, N. Veronese, G. Guglielmi, Reliability of measuring the fat content of the lumbar vertebral marrow and paraspinal muscles using MRI mDIXON-quant sequence, Diagn. Interv. Radiol. 24 (2018) 302–307.
[25] Y. Peng, W. Li, Y. Wang, et al., The cut-off point and boundary values of waist-to-height ratio as an Indicator for cardiovascular risk factors in Chinese adults from the PURE study, PLoS One 10 (2015) e0144539.
[26] Y. Zhang, Z. Zhou, C. Wu, D. Zhao, C. Wang, X. Cheng, W. Cai, L. Wang, Y. Duanmu, C. Zhang, W. Tian, Population-stratified analysis of bone mineral density distribution in cervical and lumbar vertebrae of Chinese from quantitative computed tomography, Korean J. Radiol. 17 (2016) 581–589.
[27] J.M. Bland, D.G. Altman, Statistical methods for assessing agreement between two methods of clinical measurement, Lancet 1 (8476) (1986 Feb 8) 307–310.
[28] T.R. Johnson, Dual-energy CT: general principles, Am. J. Roentgenol. 199 (5 Suppl) (2012 Nov) S3–S8.
[29] P.I. Mallinson, T.M. Coupal, P.D. McLaughlin, S. Nicolaou, P.L. Munk, H.A. Ouellette, Dual-energy CT for the musculoskeletal system, Radiology 281 (2016) 690–707.
[30] X-ray Mass Attenuation Coefficients. NIST Standard Reference Database 126. Tables of X-ray Mass Attenuation Coefficients and Mass Energy-Absorption Coefficients from 1 keV to 20 MeV for Elements Z = 1 to 92 and 48 Additional Substances of Dosimetric Interest, National Institute of Standards and Technology, Gaithersburg, MD, 2004 20899. Available online: https://www.nist.gov/pml/x-ray-mass-attenuation-coefficients , Accessed date: 13 December 2018.